Equation of state of α-Al$_2$O$_3$

A. Dewaele and M. Torrent

CEA, DAM, DIF, 91297 Arpajon Cedex, France

The ambient temperature equation of state of ruby in the corundum phase (α-Al$_2$O$_3$) has been measured up to 165 GPa in a diamond anvil cell, using a soft pressure transmitting medium. No clear sign of phase transformation or amorphization has been observed in this range, which could affect its luminescence signal. The equation of state of α-Al$_2$O$_3$ has also been calculated within density functional theory, with two different approximations of the exchange-correlation energy (local density and generalized gradient). With suitable correction, these equations of state are predictive within $\Delta P/P = 2.5\%$.

I. INTRODUCTION

Corundum (α-Al$_2$O$_3$, space group R-3c) is an important material for high pressure technologies. It is used as a window in shock-wave experiments. Doped with Cr^{3+}, it is called ruby and among other uses, it is a secondary pressure gauge in diamond anvil cell experiments.[1] The shift of the ruby luminescence wavelength with pressure has been calibrated using the equation of state of several metals, reduced from shock wave conditions to 300 K, up to 160 GPa.[1–3] Because of its easy laboratory use, its chemical inertness, and its large commercial availability, ruby is the most common pressure gauge in diamond anvil cell technology. Its physical properties under pressure have been reviewed in Ref. 4.

It has been theoretically predicted[5] and experimentally checked[6] that the thermodynamically stable phase of Al$_2$O$_3$ above $\simeq$95 GPa has a Rh$_2$O$_3$ (II) structure. The corundum and Rh$_2$O$_3$ (II) crystalline structures are close, with six-coordinated Al atoms and four-coordinated O atoms. A mechanism for the transformation has been proposed, which verifies the experimental finding that heating above $\simeq$1200 K[7] is necessary to overcome its kinetic barrier.[8] Above 130 GPa and with heating, another phase of alumina has been synthesized, which has a post-perovskite structure.[9,10]

It has been suggested that even if they are kinetically hindered, the phase transformations in alumina could influence its high pressure/ambient temperature properties. A significant redshift and broadening have been observed in the luminescence spectrum of α-Al$_2$O$_3$:Cr^{3+}, back transformed from the Rh$_2$O$_3$ (II) structure to the corundum structure by pressure release.[7] Lin *et al.* suggest that the ruby pressure scale needs to be re-examined in the high-pressure phase stability field. It has also been proposed that Al$_2$O$_3$ becomes progressively amorphous by cold compression above 95 GPa.[11]

X-ray diffraction studies of ruby under pressure at 300 K have been scarce. In 1988, the corundum phase was observed up to 175 GPa using the energy-dispersive technique.[12] Its equation of state (EoS) has been measured up to 50 GPa by compression in an argon pressure transmitting medium.[13] We are not aware of any work which would have taken advantage of the recent advances in high pressure technologies (pressurizing conditions; x-ray diffraction) to better constrain the stability field and EoS of ruby at high pressure and 300 K. However, a reference EoS is needed to use ruby—which is almost always present in the high pressure chamber of

a diamond anvil cell—as an X-ray pressure calibrant. This would be particularly useful above 1 Mbar, when the ruby luminescence signal decreases.

We report here *P-V* data for ruby single crystals compressed in helium pressure transmitting medium at ambient temperature in a diamond anvil cell. These data show that ruby remains metastably in the corundum phase up to 165 GPa; the pressure effect on the luminescence signal is reversible. *P-V* points are also calculated using density functional theory and the accuracy of these calculations is discussed.

II. EXPERIMENTAL METHODS

Three x-ray diffraction experiments have been performed with a similar sample geometry. One single crystalline ruby sphere (provided by RSA-le Rubis) was loaded in a helium pressure transmitting medium together with various metals,[3,14] which EoS was measured. The pressure was determined using ruby luminescence.[15] The size of the ruby spheres was chosen so that they were not directly compressed between the diamond anvils in the course of the experiment. Membrane diamond anvil cells with large x-ray aperture, ensured by the use of boron nitride diamond supports, have been used. The monochromatic x-ray signal diffracted by the ruby sample has been collected on a MAR imaging plate system, located at a distance of $\simeq$400 mm from the sample, on the ID27 or ID09 beamlines of the European Synchrotron Radiation Facility. The sample was rotated by $\pm10°$ during data collection. The diffraction geometry was determined using a silicon or LaB$_6$ reference sample. Several single crystal x-ray diffraction peaks (4 to 8) of ruby were individually integrated using the FIT2D software and used to determine the lattice parameters of α-Al$_2$O$_3$.

III. METASTABILITY OF α-Al$_2$O$_3$

Figure 1 presents the evolution of the width of the diffraction angle of two peaks of α-Al$_2$O$_3$ during the highest pressure run. This width increases with pressure above $\simeq$80 GPa, and is roughly doubled at 165 GPa, which is generally interpreted as a signature of nonhydrostatic compression.[16] However, 80 GPa is close to the pressure at which the Rh$_2$O$_3$ (II) becomes the thermodynamically stable phase (96 GPa).[7] The increase of the x-ray diffraction peaks could thus be a sign of a minor disorder on the way to amorphization. However, ruby remains crystalline up to 165 GPa at 300 K. Our data thus confirm the
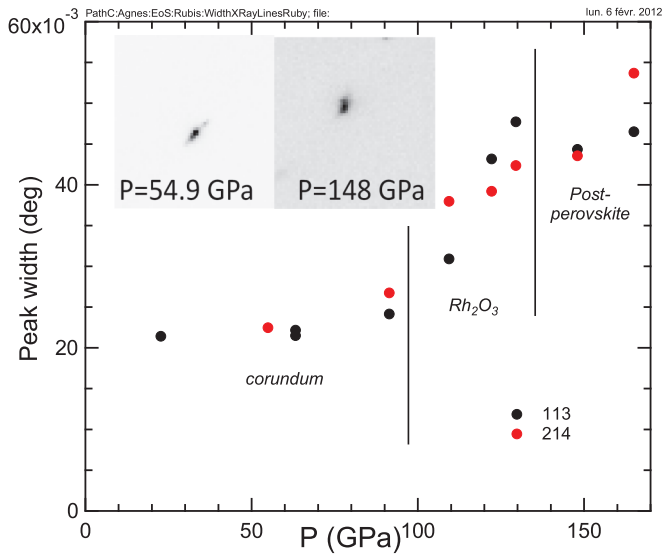
FIG. 1. (Color online) Evolution of the width (in 2θ) of two x-ray diffraction peaks of ruby in the corundum structure (R-$3c$) in the highest pressure run. The domains of thermodynamic stability of the phases of alumina (corundum R-$3c$, Rh_2O_3 (II) *Pbcn*, post-perovskite *Cmcm*) are indicated. Inset: (214) x-ray diffraction peak at two different pressures.

FIG. 2. (Color online) Ruby luminescence spectra recorded after complete decompression, for one ruby ball compressed to more than 180 GPa (top) and one ruby ball compressed to 10 GPa (bottom).

finding of Jephcoat *et al.*,[12] but on the basis of more accurate x-ray diffraction data.

It has been proposed that compressing ruby beyond the stability domain of α-Al_2O_3 (0–96 GPa) could influence the pressure shift of the ruby luminescence line.[6,7] When the corundum structure is recovered from the Rh_2O_3 (II) structure upon decompression, a remanent effect (e.g., a broadening and a redshift of the luminescence maximum corresponding to a "fossilized" pressure of 5.03 GPa) on ruby luminescence has been observed.[7] This raises the question: Does a similar effect exists at ambient temperature, which would affect the ruby luminescence signal above $\simeq 100$ GPa? We have recovered a ruby after cold nonhydrostatic compression to more than 180 GPa in a nonhydrostatic environment. Its luminescence spectrum is presented in Fig. 2 and compared to a luminescence spectrum obtained after decompression to only 10 GPa. While compression to 10 GPa does not affect the position and the width of the luminescence lines, compression to 180 GPa results in a doubling of their width and a shift of their position. However the broadening is not as important as the one reported in the Lin *et al.* study. The "fossilized" pressure, i.e., the remanent redshift is only 0.4 GPa. We thus conclude that ambient temperature compression of ruby up to 200 GPa only marginally affects pressure measurement by the ruby luminescence technique.

IV. COMPARISON BETWEEN EXPERIMENTAL AND THEORETICAL EOS

The a and c lattice parameters determined by a least-square fit of the x-ray diffraction peak distances are summarized in Table I. The P-V data points are presented in Fig. 3. The measurements performed in three different experimental runs agree with each other, although the data taken during run 2 appear more scattered. This is due to the lower number
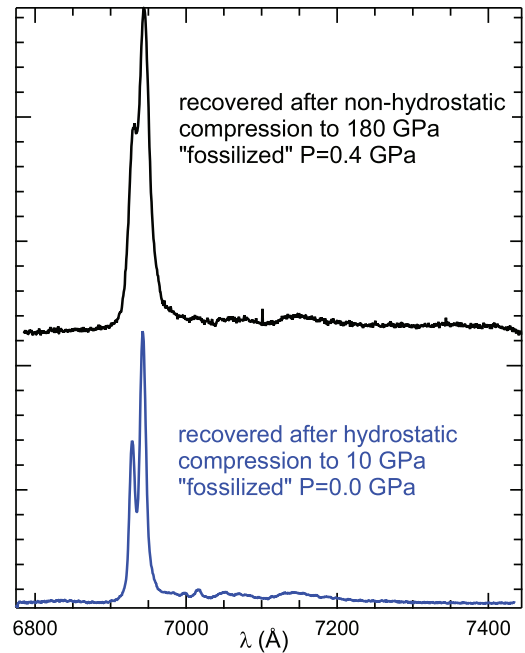
of diffraction peaks followed in this run. The measurements found in the literature[12,13,17] are plotted on the same graph. With increasing pressure, the volumes measured by previous studies become higher than the volumes measured here. It illustrates the effect of nonhydrostatic stress on EoS measurements. In fact, Jephcoat *et al.* compressed ruby without any pressure medium (which leads to a large overestimation of volume),[16] and Richet *et al.* and Dubrovinsky *et al.* compressed ruby in less hydrostatic pressure media than helium (which leads to an overestimation of volume above several GPa).[16] When the current points are fitted by a Rydberg-Vinet EoS formulation,[18] the following parameters are obtained: $V_0 = 255.45 \pm 0.52$ Å^3 (volume under ambient conditions), $K_0 = 254.1 \pm 7.6$ GPa (bulk modulus under ambient conditions), $K_0' = 4.00 \pm 0.15$ (its pressure derivative). The uncertainties given here correspond to the 95% confidence interval for fit coefficients. The fitted K_0 is in very good agreement with the isothermal bulk modulus obtained from ultrasonic experiments[4] ($K_{0\,US} = 253 \pm 2$ GPa). Its pressure derivative K_0' is slightly lower ($K_{0\,US}' = 4.30 \pm 0.15$). The c/a parameter decreases continuously with pressure.

Information on the athermal EoS of α-Al_2O_3 calculated using density functional theory can be found in the literature. This EoS should be very close to the measured EoS at 300 K, the zero-point pressure and thermal pressure correction being small. Theoretical V_0, K_0, and K_0' found in the literature are listed in Table II. In Ref. 9, P-V points have been calculated within local density approximation (LDA) and generalized gradient approximation (GGA) using norm-conserving pseudopotentials, and a plane-wave basis is provided every 60 GPa up to 240 GPa. The Perdew-Burke-Ernzerhof[19] (PBE) functional has been used for GGA. The use of pseudopotential implies that respectively 10 and 2 core electrons have been frozen for Al and O and that "pseudo" quantities have been

TABLE I. Lattice parameters of ruby measured by x-ray diffraction together with the pressure from ruby luminescence (Ref. 15) in three experimental runs. The data are listed in the order they have been taken (in general, on pressure increase). The volume of the unit cell plotted in Fig. 3 is $V = a^2 c \sqrt{3}/2$.

P (GPa)	a (Å)	c (Å)	P (GPa)	a (Å)	c (Å)
Run 1			50.6	4.5399	12.379
22.7	4.645	12.627	55.3	4.5267	12.298
28.8	4.620	12.563	59.8	4.5122	12.262
49.1	4.540	12.326	66.3	4.4926	12.192
54.9	4.523	12.268	72.4	4.476	12.068
63.2	4.499	12.192	77.3	4.4637	12.079
69.2	4.482	12.138	82.3	4.4513	12.000
74.6	4.471	12.088	**Run 3**		
79.3	4.451	12.054	1.32	4.7524	12.991
91.4	4.424	11.972	1.9	4.7509	12.964
97.5	4.411	11.926	2.4	4.7481	12.964
103.8	4.400	11.886	3.45	4.7436	12.946
109.4	4.388	11.845	3.85	4.7412	12.942
115.6	4.370	11.802	5.90	4.7301	12.899
122.2	4.352	11.77	7.25	4.7222	12.875
129.5	4.343	11.702	8.90	4.7088	12.854
136.3	4.329	11.651	11.0	4.7003	12.824
144	4.314	11.619	12.55	4.6897	12.824
148	4.306	11.586	15.65	4.6750	12.764
153	4.293	11.577	17.7	4.6656	12.729
159	4.283	11.538	20.2	4.6546	12.698
165	4.275	11.501	22.8	4.6433	12.648
Run 2			25.1	4.6338	12.627
22.2	4.6508	12.668	27.6	4.6222	12.584
29.3	4.6195	12.581	30.2	4.6133	12.565
32.0	4.6072	12.551	32.5	4.6040	12.530
36.7	4.5894	12.498	36.0	4.5896	12.482
42.0	4.5687	12.477	0.56	4.7565	12.998

used out of the core region in the calculations. We have fitted these points with a Rydberg-Vinet EoS to obtain the parameters presented in Table II. Rydberg-Vinet parameters obtained using LDA and the plane-wave norm-conserving pseudopotential method were directly provided in Ref. 10. In Ref. 20, equilibrium volume and bulk modulus have been calculated within LDA or GGA, also using norm-conserving pseudopotentials and plane waves. One LDA all-electron EoS calculation—using the linear combination of Gaussian type orbitals-fitting function (LCGTO-FF)—has been published,[21] which explicitly takes into account all electrons of O and Al. The equilibrium volume, 255 Å^3, is close to the experimental one; however, lattice parameters and atomic positions have not been fully relaxed. The equilibrium volume is around 243 Å^3 for two pseudopotential studies.[9,20] Surprisingly, in another reference,[10] apparently identical methods (same approximations, pseudopotentials and basis) to Ref. 9 lead to $V_0 = 255$ Å^3.

The published theoretical EoS of α-Al$_2$O$_3$ thus appear relatively scattered; it can be attributed to the variety of approximations and methods used (frozen-core, pseudopotential, LDA/GGA, structural relaxation,...). We have thus performed additional calculations, with the most accurate method and convergence parameters, using the ABINIT package.[22] The
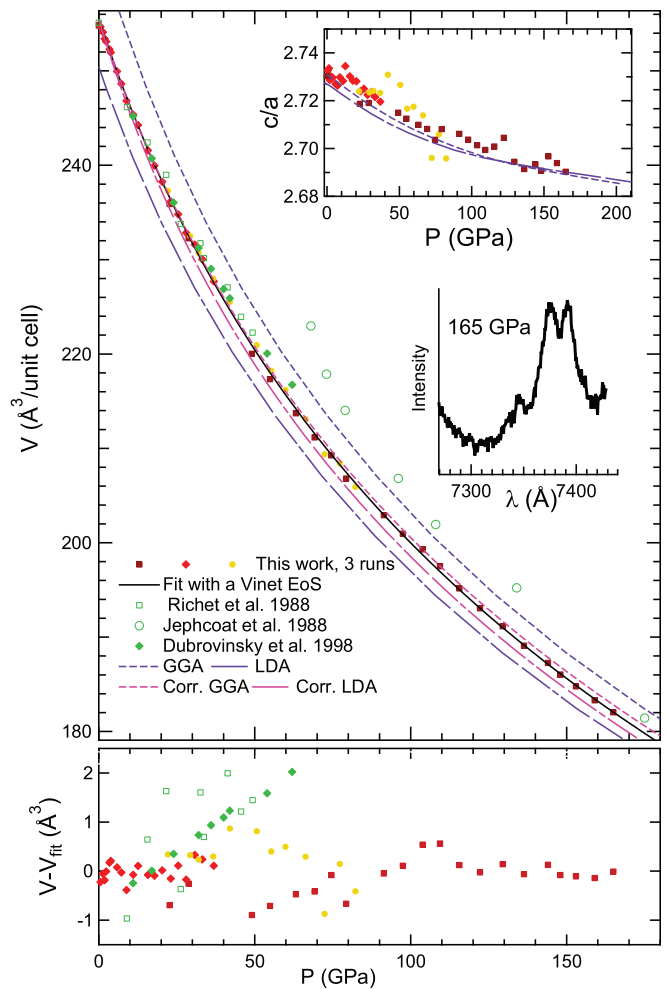
FIG. 3. (Color online) (Top graph) Volume of the hexagonal cell (6 formula units) and c/a ratio measured ruby in the corundum structure as a function of pressure. The current data points and literature experimental data points are presented. The ruby fluorescence spectrum recorded at the highest pressure reached in this study, 165 GPa, is plotted as a second inset. The P-V points calculated within density functional theory in this study (PBE-GGA-PAW, LDA-PAW) and corrected forms (see text) are also plotted. (Bottom graph) Volume difference between raw data points and the fitted form: Vinet EoS with $V_0 = 255.45$ Å^3/hexagonal cell, $K_0 = 254.1$ GPa, $K_0' = 4.00$.

projector augmented-wave (PAW) method,[23,24] which is expected to be almost as accurate as all-electron methods,[14] has been used within LDA and PBE-GGA. Specific PAW data sets with small core radii and excluding semicore states from the core (2 core electrons for Al) have been generated. This ensures maximum transferability for calculations under high pressure. The Monkhorst-Pack mesh used for sampling the Brillouin zone was 10x10x10 and the plane-wave cutoff energy was 30 Ha (resp. 50 Ha) for the wave functions (resp. the augmentation charges). The lattice parameters and atomic positions have been fully relaxed, at fixed volume, giving a pressure value. 15 P-V points calculated between 0 and 200 GPa have been fitted by a Rydberg-Vinet[18] EoS; the parameters are listed in Table II. The predicted trend for relaxed c/a ratio is following very closely the experimental one (Fig. 3).

TABLE II. Rydberg-Vinet[18] EoS parameters for corundum obtained in the current study, experimentally and using density functional theory calculations. The same parameters obtained in the literature are also listed. The approximation made for the exchange correlation term, local density approximation (LDA), or generalized gradient approximation (GGA) with PBE functional is specified. The electrons treatment (all-electron-LCGTO-FF, plane-wave pseudopotentials or projector augmented wave, PAW) is also listed.

Reference	Method	V_0, K_0, K_0' ($Å^3$, GPa, no unit)	
This study	Experiments	255.45, 254.1, 4.00	
Reference	Method	$V_{0\,AbI}, K_{0\,AbI}, K_{0\,AbI}'$ ($Å^3$, GPa, no unit)	$V_0, K_{0\,AbI\,Corr}, K_{0\,AbI\,Corr}'$ ($Å^3$, GPa, no unit)
This study	LDA-PAW	250.5, 252.9, 4.251	255.45, 232.4, 4.38
This study	GGA-PBE-PAW	263.5, 224.8, 4.28	255.45, 255.3, 4.10
Ref. 21	LDA-All-electron LCGTO-FF	255.18, 243.8, 4.30	255.45, 242.7, 4.31
Ref. 9	LDA-PW-pseudo	242.9, 248.6, 4.13	255.45, 200.3, 4.46
Ref. 9	GGA-PBE-PW-pseudo	262.12, 223.8, 4.20	255.45, 248.9, 4.05
Ref. 10	LDA-PW-pseudo	254.57, 252.6, 4.24	255.45, 248.9, 4.26
Ref. 20	LDA-PW-pseudo	243.9, 261.8	255.45, 216.2
Ref. 20	GGA-PBE-PW-pseudo	255.73, 236.5	255.45, 237.9

The equilibrium volume obtained within LDA (251 $Å^3$) is relatively close to the all-electron calculation (255 $Å^3$),[21] as expected for the PAW method. The 2% difference may be attributed to the absence of relaxation of the cell in all-electron calculation.[21] Equilibrium volumes obtained with pseudopotentials[9,20] are lower than with PAW, except for one study.[10] In Ref. 9, the unusually large difference between LDA and GGA-PBE may be attributed to the small number of k points used in the calculation ($4 \times 4 \times 4$).

As observed earlier,[14] the experimental compression curve is bracketed between LDA and PBE-GGA compression curves (Fig. 3). The equilibrium volumes obtained in PBE-GGA and LDA are respectively 3% higher and 2% lower than the experimental volume, and the bulk modulus varies accordingly, a higher equilibrium volume leading to a lower bulk modulus (Table II).

It has been proposed that the predictive power of density functional theory-based EoS can be drastically improved by correcting them using information provided by experiments.[4,14,25] In Ref. 4, it is found that all theoretical EoS merge when they are scaled ($P/K_{0\,AbI}$ vs $V/V_{0\,AbI}$); in other words, all DFT calculations yield similar K_0', which can be checked in Table II. However, the theoretical value of K_0' (4.30 in average) is slightly higher than the experimental one (4.00). We follow here the method proposed in Ref. 14 based on data on several metals. This method uses a set of three new parameters to generate a corrected Rydberg-Vinet EoS: $V_{0\,exp}$ (experimental equilibrium volume), $K_{0\,AbI\,Corr}$, and $K_{0\,AbI\,Corr}'$. The last two parameters (bulk modulus and its pressure derivative) are calculated using *ab initio* Rydberg-Vinet EoS $P_{AbI}(V)$. They express as: $K_{0\,AbI\,Corr} = -V\,\partial P_{AbI}/\partial V(V_{0\,exp})$ and $K_{0\,AbI\,Corr}' = V^2/K\,\partial^2 P_{AbI}/\partial V^2(V_{0\,exp})$. Corrected moduli for corundum are listed in Table II. When not available in the calculation, a K_0' value of 4.0 has been assumed to establish the correction for $K_{0\,AbI}$ and $K_{0\,AbI}'$. The corrected bulk moduli obtained within LDA are lower than the experimental one and the difference is significant (more than 15%) for pseudopotential studies.[9,20] However, the corrected bulk moduli obtained with GGA-PBE-PAW and LDA-PAW remain close to the experimental one. For a given volume, the corrected GGA-PBE-PAW and LDA-PAW pressures are within $\pm 2.5\%$ of experimental pressure up to 160 GPa (Fig. 3); this difference is of the same order of magnitude as the uncertainty on pressure gauges such as ruby calibration in diamond anvil cells.[14] Corundum thus appears as an additional material for which density functional theory based EoS can be predictive, with the suitable correction.

V. CONCLUSION

The EoS of corundum (α-Al_2O_3) has been measured up to 165 GPa at 300 K, under quasihydrostatic compression (with helium pressure transmitting medium) in a diamond anvil cell. We have obtained the following Rydberg-Vinet parameters: $V_0 = 255.45 \pm 0.52$ $Å^3$/hexagonal cell, $K_0 = 254.1 \pm 7.6$ GPa, $K_0' = 4.00 \pm 0.15$. They can be used for pressure calibration purposes. Even if the corundum phase is only metastable above $\simeq 96$ GPa, we do not report any amorphization or luminescence red line shift for this material up to at least 165 GPa. We have also tested the ability of density functional theory calculations to predict the corundum EoS. They have been performed with the plane augmented wave method using two approximations (LDA and PBE-GGA). The calculated equilibrium volumes are within -2% (LDA) to $+3\%$ (PBE-GGA) of experimental volume. We show that when the volume, bulk modulus, and its pressure derivative are corrected using the equilibrium volume as the only experimental input, the theoretical equation of state becomes predictive within $\Delta P/P = 2.5\%$ in the scanned pressure range.

[1]H. K. Mao and P. M. Bell, J. Appl. Phys. **49**, 3276 (1978).

[2]H. Mao, J. Xu, and P. Bell, J. Geophys. Res. **91**, 4673 (1986).

[3]A. Dewaele, P. Loubeyre, and M. Mezouar, Phys. Rev. B **70**, 094112 (2004).

[4]K. Syassen, High Press. Res. **28**, 75 (2008).

[5]R. E. Cohen, Geophys. Res. Lett. **14**, 1053 (1987).

[6]N. Funamori and R. Jeanloz, Science **278**, 1109 (1997).

[7]J.-F. Lin, O. Degtyareva, C. T. Prewitt, P. Dera, S. Nagayoshi, E. Gregoryanz, H.-K. Mao, and R. J. Hemley, Nat. Mater. **3**, 389 (2004).

[8]B. Xu, H. Stokes, and J. Dong, J. Phys.: Condens. Matter **22**, 315403 (2010).

[9]R. Caracas and R. E. Cohen, Geophys. Res. Lett. **32**, L06303 (2005).

[10]A. Oganov and S. Ono, Proc. Nat. Acad. Sci. USA **102**, 10828 (2005).

[11]W. J. Nellis, Phys. Rev. B **82**, 092101 (2010).

[12]A. P. Jephcoat, R. J. Hemley, and H. K. Mao, Physica B **150**, 115 (1988).

[13]P. Richet, J.-A. Xu, and H.-K. Mao, Phys. Chem. Miner. **16**, 207 (1988).

[14]A. Dewaele, M. Torrent, P. Loubeyre, and M. Mezouar, Phys. Rev. B **78**, 104102 (2008).

[15]P. I. Dorogokupets and A. R. Oganov, Phys. Rev. B **75**, 024115 (2007).

[16]A. Dewaele and P. Loubeyre, High Press. Res. **27**, 419 (2007).

[17]L. S. Dubrovinsky, S. K. Saxena, and P. Lazor, Phys. Chem. Miner. **25**, 434 (1998).

[18]P. Vinet, J. Ferrante, J. R. Smith, and J. H. Rose, J. Phys.: Condens. Matter **19**, L467 (1986).

[19]J. P. Perdew, K. Burke, and M. Ernzerhof, Phys. Rev. Lett. **77**, 3865 (1996).

[20]S. Jahn, P. A. Madden, and M. Wilson, Phys. Rev. B **74**, 024112 (2006).

[21]J. C. Boettger, Phys. Rev. B **55**, 750 (1997).

[22]X. Gonze *et al*., Comput. Phys. Commun. **180**, 2582 (2009).

[23]P. E. Blöchl, Phys. Rev. B **50**, 17953 (1994).

[24]M. Torrent, F. Jollet, F. Bottin, G. Zérah, and X. Gonze, Comput. Mater. Sci. **42**, 337 (2008).

[25]K. Kunc and K. Syassen, Phys. Rev. B **81**, 134102 (2010).